Istraživanja i projektovanja za privredu
ISSN 1451-4117
DOI:10.5937/jaes0-40421
www.engineeringscience.rs

iipp publishing

Journal of Applied Engineering Science
Vol. 21, No. 2, 2023
Original Scientific Paper
Paper number: 21(2023)2, 1091, 470-480

ROLL DYNAMIC COEFFICIENTS APPROACH OF DECAY TEST USING THE GENERALIZED REDUCED GRADIENT METHOD (GRG)

Hasanudin[1], Achmad Zubaydi[2]*, Wasis Dwi Aryawan[2]

[1]PhD Student of Naval Architecture, Faculty of Marine Technology, Institut Teknologi Sepuluh Nopember (ITS), Keputih, Sukolilo, Surabaya City, East Java, Indonesia
[2]Department of Naval Architecture, Faculty of Marine Technology, Institut Teknologi Sepuluh Nopember (ITS), Keputih, Sukolilo, Surabaya City, East Java, Indonesia

* zubaydi@na.its.ac.id

Sea transportation is the vehicle which dominant and vital in the world. The increasing number of ships, types, and uncertain climate change have caused many ship accidents that have caused loss of life and property. The International Maritime Organization (IMO) issued the latest regulation on the second generation of ship stability criteria based on the dynamic of ship roll motions. The survival of dynamic stability depends on the hydrodynamic coefficients, which numerical and experimental calculations can obtain. The problem is finding the hydrodynamic coefficients of the ship roll quickly and accurately from the experimental roll decay data. This paper uses the Generalized Reduced Gradient (GRG) optimization to find the roll motion coefficient with the objective function of a standard deviation. The results show that the roll decay experiment graph is close optimization for variations of the minimum standard deviation used: all data, maximum-minimum amplitude, maximum amplitude, and minimum amplitude. The most similar chart to the experiment is optimization using a standard deviation of maximum-minimum amplitude with the optimal objective function σ = 1.006776 closest σ=1; obtained variable $x_1 = k_{44}$ =0.1087688 m; $x_2 = B_{44}$ =3.00306E-05 m-ton-sec. Based on sensitivity tests for various scenarios, optimization with a standard deviation of maximum amplitude has a high sensitivity, so it is necessary to avoid or be careful in its use. Generally, the GRG optimization method has the advantage of finding the hydrodynamic roll coefficient quickly and accurately.

Keywords: ship, roll decay, hydrodynamic coefficients, optimization

1 INTRODUCTION

Sea transportation is an essential part of human life and domination almost 80% of the transportation modes in the world, especially in global trade and business, according to the United Nations Conference on Trade and Development (UNCTAD) [1]. The ship is the central part of the sea transportation mode that can move > 10 billion tons of containers, tangible goods, and liquid goods from one port to another regularly around the world [2]. The increasing world business system and the wide of marine exploration require many ships of various types and sizes; the negative effect of this situation causes a high risk of accidents at sea [3]. Cargo ships dominate accidents worldwide, but RoPax is the most significant loss of life that RoPax can transport goods, vehicles, and people simultaneously. These accidents often occur in developing countries such as Bangladesh, the Philippines, and Indonesia [4], [5]. The causes of accidents can come from one or a combination, and the reasons can be: human error, ship worthiness, and lousy weather [6]. Ship stability is one of the most frequent internal ship problems that can cause ships to capsize and sink on seabed [7].

IMO as a world body dealing with maritime issues, it is concerned about safety issues [8]. Ship stability is one of the essential components of safety that should be met before and when the ship operates at sea [9]. To ensure the safe stability of vessels, IMO makes general and specific stability criteria based on the type of ship [10]. This IMO stability criterion adopts Rahola's study using the energy balance moment of the ship righting arm principle and comparing this principle with statistical data of ships that survive and capsize so that the standard criteria are obtainable [11] [12]. The IMO criteria were developed not only for calm weather conditions but expanded for terrible weather conditions with the introduction of the weather criteria [13]. Subsequent developments issued particular stability criteria based on the types of new ships that are increasingly varied [14] [15]. The ship capsizing process occurs not only under static but also on dynamic conditions [16]. Considering these conditions, IMO introduced the Second Generation Intact Stability (SGIS) associated with the movement: surf riding/broaching, parametric rolling dan dead ship [17]. After going through a lengthy study, mathematical development, and experimentation, the SGIS was finalized for implementation in the seventh session of the International Maritime Organization (IMO) sub-committee on Ship Design and Construction (SDC) [18].

In dynamic conditions, the most dominant is the roll motion of the ship, which can cause the vessel to capsize [19]. The hydrodynamic coefficients of the ship strongly influence the roll motion: inertia moment, damping moment, restoring moment, and excitation moment [20]. The roll motion coefficients are obtainable using numerical calculations and roll decay experiments in the laboratory [21][22]. The procedure for obtaining accurate hydrodynamic coefficients is with the roll decay experiment contained in the manual ITTC 7.5-02-07-04.1 [23]. The reduction in data record results of the roll decay experiment obtains hydrodynamic coefficients conventionally by using the functions: roll period, ship MG, and ship displacement. The damping moment can be obtained by looking for the trend line

between the rolling amplitude of each roll movement and the decrease in the amplitude of each ship movement [24] [25]. This conventional method is less than optimal and effective for approaching a motion that rolls with infinite amplitudes.

The optimization method is reliable for finding the optimal value of a predetermined function and is applicable in various engineering fields [26]. Generally, two approaches to linear and nonlinear optimization methods were practical for dynamic motion trajectories [27]. The nonlinear GRG optimization is used in this paper because this technique is relatively more straightforward compared to other conventional methods. It is excel-based that requires a short time and few inputs to optimize a design to obtain the minimum construction cost [28] [29]. The method can also find the optimum value quickly but accurately with predetermined limits. Before calculating the optimization, it is necessary to determine the objective functions, variables, constraints, parameters, and constants [30]. In this paper, the objective functions use the standard deviation of the difference between experimental results and calculations. The variables are the arms of the roll moment of inertia and the damping moment. The limitation of the parameters is displacement and MG of the ship, while the constants used are gravity acceleration and the density of water. The equation used is duffing equation for uncoupled motion converted into an analytical trigonometric-exponential equation.

2 MATHEMATICAL MODELING

2.1 Mathematical model of motion equation and coefficient motion roll

A floating body motion naturally occurs in six degrees of freedom consisting of three translational motions (sway, heave, surge) and three rotational oscillatory (roll, pitch, yaw) [31]. Ship stability is a part of the roll motion which occurs in the couple and uncoupled motion. The roll motion of the uncouple vessel is a derivation from Newton's 2nd law of translational motion force, which change in rotational motion [32]. The restoring moment is added to accommodate oscillatory motion. Furthermore, the damping moment must be taken to reduce oscillatory motion. The excitation moment represents the oscillatory in regular and irregular waves [33]. The uncoupled equation roll motion of a periodic wave is as follows:

$$I_{44}\ddot{\phi} + B_{44}\dot{\phi} + C_{44}\phi = M_{44}Sin(\omega t) \quad (1)$$

The description of the above equation (1) is as follows: I_{44}= inertia and added moment of ship weight; $I_{44} = I_{xx} + I'_{added\ xx}$; I_{xx}= moment of ship weight; $I'_{added\ xx}$= added moment of water; $\ddot{\phi}$= roll acceleration motion; B_{44}= damping moment; C_{44}= restoring moment of the ship; $\ddot{\phi}$= roll accelerated motion; $\dot{\phi}$= roll velocity motion; ϕ= roll motion; M_{44} = excitation moment of the waves; $Sin(\omega t)$ = wave oscillatory on the regular waves. Both I_{44} and B_{44}, are the roll motion coefficients from the roll decay experiment [34] [35]. Roll decay is ship motion without excitation moment which M_{44} = 0 and ϕ_0= initial roll decay angle, so the equation (1) is solved as exponential function equation (2) (3) (4) as follows:

$$\phi = e^{vt}\left(C \cdot Cos(\omega_d t) + D \cdot Sin(\omega_d t)\right) \quad (2)$$

$$\phi = e^{\frac{B_{44}}{2 \cdot I_{44}} t}\left(\phi_0 \cdot Cos(\omega_d t) + \frac{C \cdot v}{\omega_d} \cdot Sin(\omega_d t)\right) \quad (3)$$

$$\phi = e^{\frac{B_{44}}{2 \cdot I_{44}} t}\left(\phi_0 \cdot Cos(\omega_d t) + \frac{\phi_0 \cdot \frac{B_{44}}{2 \cdot I_{44}}}{\omega_d} \cdot Sin(\omega_d t)\right) \quad (4)$$

Correlation of the damped roll frequency (ω_d), encountering frequency (ω_ϕ) and inertia moment (I_{44}) is formulated as the function of the ship metacenter $(\overline{GM}_T)$, gravity acceleration (g), ship displacement (Δ), and gyration radius of inertia moment (k_{xx}) which is formulated as follows [34] [35]:

$$\omega_d = \sqrt{{\omega_\phi}^2 - v^2}\ ;\ \omega_\phi = \sqrt{\frac{\Delta g \overline{GM}_T}{I_{44}}};\ I_{44} = 1.2\Delta k_{xx}^2\ ; \quad (5)$$

2.2 Mathematical model of optimization

Optimization is a mathematical method or program to find the best solution: the value sought is called the variables, the value to be optimized (maximum or minimum) is called the objective function, and the optimization must fulfill constraints [27]. The objective function can use a single objective or multiple objectives, and the formula is as follows:

$$\text{Minimum or Maximum } f(\vec{x}) := [f_1(\vec{x}), f_2(\vec{x}), \dots, f_k(\vec{x})\ ] \tag{7}$$

Subject to:

$$g_i(\vec{x}) \leq 0 \quad i = 1,2,\dots,m \tag{8}$$

$$h_i(\vec{x}) \leq 0 \quad i = 1,2,\dots,m \tag{9}$$

Where $\vec{x} = [\vec{x}_1, \vec{x}_2, \dots, \vec{x}_n\ ]^T$ are vector variables; $f_i,\ i = 1, \dots\dots, k$ are objective functions; and $g_i, f_i\ \ i = 1, \dots\dots, m, j = 1, \dots, p$ are constraints [36]. There are two optimization problems in the form of the function that is solved, namely, the linear problem and the nonlinear problem. One of the nonlinear optimization methods is the GRG, a robust and reliable method for solving optimization problems. There are two options for solving the GRG method using the Quasi-Newton Method and the Conjugate Gradient Method. This GRG method uses numerical mathematics with a base using the derivative of the objective function (gradient) near or equal to zero [37]. The procedure for solving the problem begins with setting the variable $x^0 = \underline{x}$, next choose step α_i with direction vector d_i so the numerical iteration variable can be formulated:

$$x_{i+1} = x_i + \alpha_i d_i \tag{10}$$

The variables obtained in equation (10) are entered into the objective function as follows:

$$optimum\ F(x_i + \alpha_i d_i) \tag{11}$$

The next step is to set the objective function to the optimum mode (choose the maximum or minimum). Further, the objective function is iterated and checked to the optimum point, where the value is at the beginning and continues the objective function iteration or the gradient close to zero. Hence the following formula:

$$\frac{dF_{i+1}}{dx_{i+1}} = \frac{(F(x_i + \alpha_i d_i) - F(x_i)}{(x_i + \alpha_i d_i) - x_i} \cong 0 \tag{12}$$

3 CASE STUDY AND METHODOLOGY

3.1 Case study of roll decay experiment

This paper uses a case study of the double-ended RoPax ship, the most famous ship in the world but contributes the most casualties. The coefficient of hydrodynamic roll motion was obtained from the roll decay experiment in the flume tank. The ship model was to represent the ship RoPax Windu Karsa which operated in the Bojoe-Kolaka route in Indonesia water. The flume tank with dimensions size is (20 x 2.3 x 2.5) meters, and the water depth was set up at 0.7 meters. The ship model is made to scale 1:42, or the length of the model is 1.36 m; this length is determined by considering when the model was placed transversely in the flume tank. There was still a clearance of 0.57 m in front and behind the model to the wall so that when the roll test was carried out, the water did not bounce to the model, which can interfere with experimental accuracy results. The model scale and test procedure size refer to ITTC 7.5-02-07-04.1 [23]. The main dimensions of RoPax and the model shown in Table 1 are as follows:

Table 1. Main dimensions of RoPax and model

Dimension Item	RoPax		Model	
Length overall (Loa)	57.20	M	1.36	m
Length perpendicular (Lpp)	49.66	M	1.24	m
Breadth (B)	16.20	M	0.39	m
Height (H)	3.80	M	0.09	m
Draft (T)	2.92	M	0.0695	m
Model scale	1		42	

The ship used in the experiment was a double-ended RoPax with the same after and forward shape so that the effect of motion other than roll is small. Then, make the ship hull model according to the line plan and set the shipload with the same complete draft of the existing ship. The displacement was 11.2 kg consisting of the ship hull model and portable ballast, and high KG = 11.00 cm. The shape of the hull and its placement in the flume tank can be seen in Fig. *1* as follows:

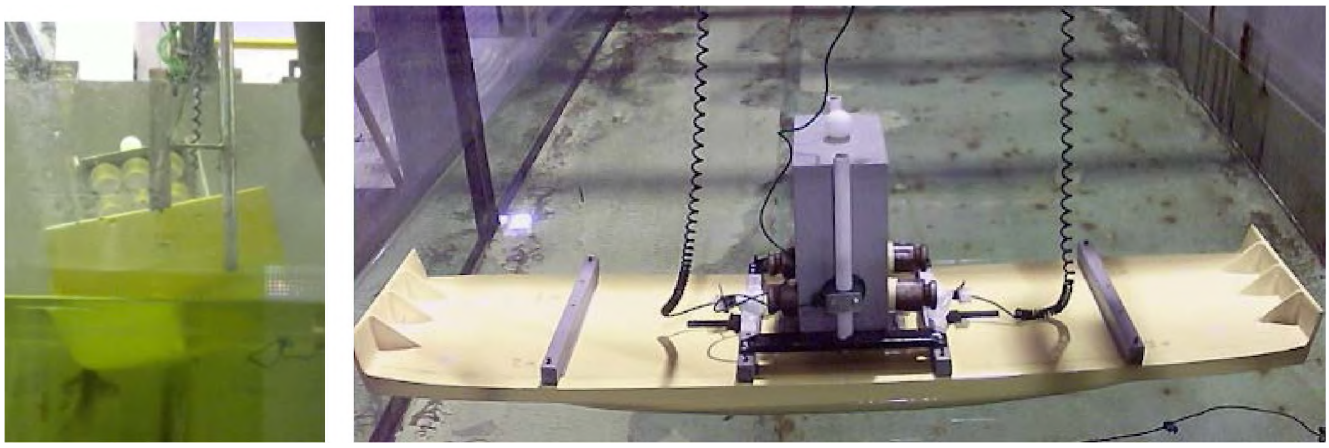

Fig. 1. Setting of roll decay test with initial angle ±20 degree in the flume tank

The experiment process was by placing the ship model in calm water transversely in a flume tank, and then 2 (two) gyroscope sensors were installed to record the ship roll. The initial heel of a ship is set up ±20 degrees, as shown in Fig. 1, by using a rope hook tied around the hull. The rope was released to allow the rolling oscillation motion to occur, and the sensor recorded the roll motion until it stopped. The recorded data was filtered to obtain accuracy and be free from noise.

3.2 Optimization methodology

Getting the coefficients of roll motion from the experimental record is carried out using the GRG optimization. The optimization components determine the methodology for solving optimization problems [38]. Classification of optimization components is fundamental and is one of the main parts of solving optimization problems. The type of optimization components in this problem is as follows:

Variables: $x_1 = k_{xx}$

$x_2 = B_{44}$

Objective Function:

$$\text{minimum } \sigma = \sqrt{\frac{\sum_i^n (\phi_{i.exp} - \phi_{i.cal})^2}{(n-1)}} \quad (13)$$

σ = deviation standard

$\phi_{i.exp}$ = roll decay record

$\phi_{i.cal}$ = roll decay calculation (refer to equation 4)

n= number of samples used

Parameters: Δ, $\overline{GM}_T$ (based on weight measurement and inclining test)

Constants: g, ρ (Physical constants)

Constraints: $0.25B \leq k_{xx} \leq 0.4B$; or

$1.2\Delta(0.25B)^2 \leq I_{44} \leq 1.2\Delta(0.4B)^2$

B=ship model breadth;

k_{xx}= weight gyration of inertia moment

After classifying, the mathematical model is constructed using spreadsheet Microsoft Office Excel. The GRG method used in this optimization [38], as shown on the right in Fig. 2. The first raw show the setting cell of objective (σ); the second row is minimized setting of the objective function; the third row are variables setting (k_{xx} dan I_{44}); the fourth is constraints setting (k_{xx} dan I_{44}); the end chose the GRG nonlinear to solve the optimization model. The left below Fig. 2 shows the final convergent solution, marked with all the constraints satisfied; the objective function is minimized and will be written: “solver found a solution”.

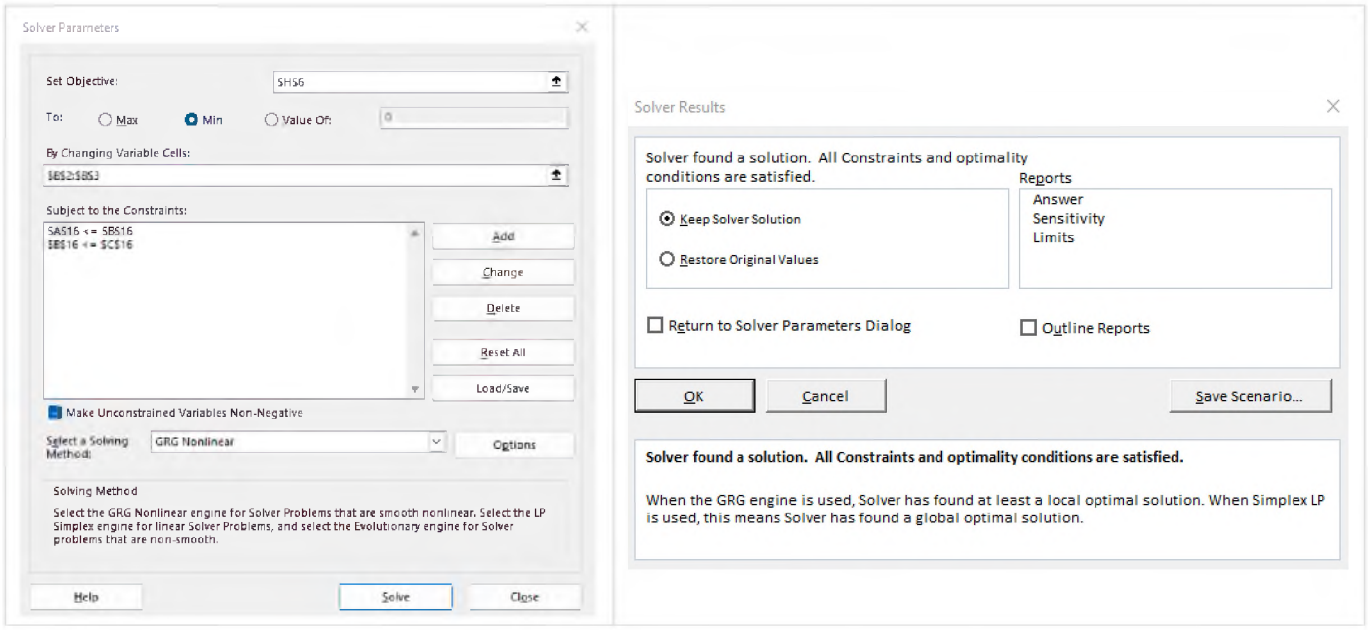

Fig. 2. Setting solver and result optimization in Microsoft office excel

4 DISCUSSION

From the experiment roll decay record, the motion can be approximated by equations 1~4. Next, the mathematical optimization models using section 3.2 are applied. The initial variables of the coefficient of the inertia moment gyration radius and damping moment are determined. Then type optimization software is carried out using nonlinear GRG optimization by varying standard deviation of the sample record data obtained as described below:

4.1 The objective function uses a standard deviation of all data roll decay

At the beginning of the experiment, the ship model is set up on the initial heel of 20.830 degrees ≅ 20 degrees in calm water. Next, the model is released so that the rolling oscillates, which gets smaller and smaller until the oscillation stops. The oscillating movement of the ship model is made free-floating without a tie. The results of the roll decay experiment data are shown in Fig. 3 of the dashed black curve as follows:

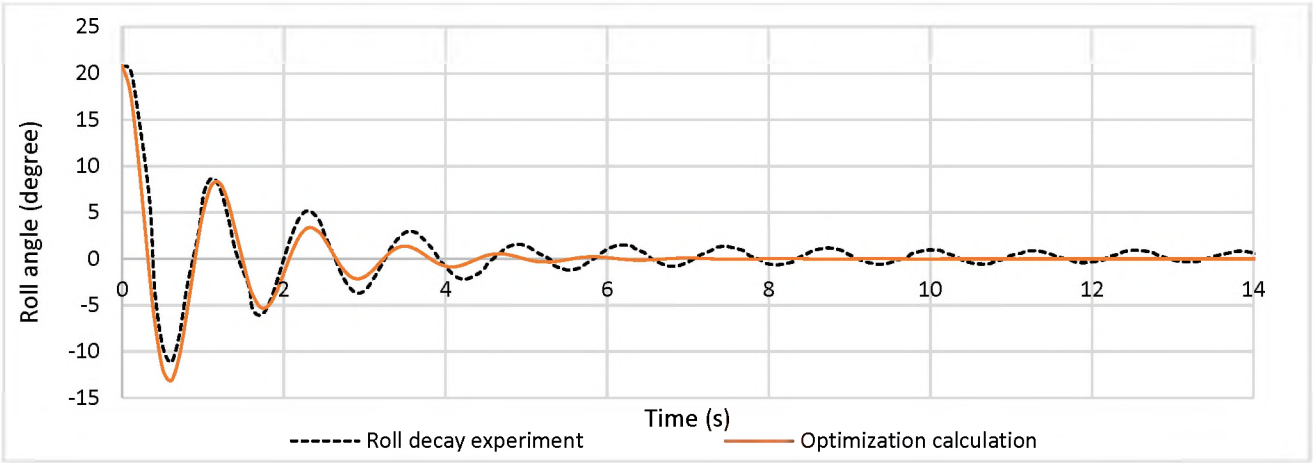

Fig. 3. Comparison of experiment with optimization using a standard deviation of all roll decay data

Fig. 3 shows the similarity of roll decay curves experiment with the dashed black curve and optimization calculation using the objective function of all roll decay data with the solid orange curve. The similarity curve starts from oscillatory time 0 to 2.116 seconds; the slightly different times 2.116 -5.944 seconds and deviation are even more significant at times above 5.944 seconds. In addition to comparing experimental and optimization results displayed in curves, it can also be displayed in the form of data, as shown in Table 2. The first row is the number of data records from gyrocompass sample 150 data, the second row of the record time range 0-15.01 seconds, and the third row is the row roll angle decay. In addition, the calculation of roll decay analytically is carried out by entering the same time interval as the experimental results shown in the fourth row.

Table 2. Comparison of experiment with optimization using a standard deviation of all roll decay data

Data (n)	1	2	3	4	5	6	7	.....	150
t (s)	0	0.1	0.202	0.34	0.503	0.604	0.706	.....	15.01

Data (n)	1	2	3	4	5	6	7	.....	150
$\theta_{i.exp}$(deg)	20.830	20.435	15.381	6.158	-9.503	-11.161	-8.262	.....	0.6757
$\theta_{i.cal}$(deg)	20.830	17.967	10.523	-1.918	-11.96	-13.145	-10.531	.....	0.0012

All the experimental data of rows 1-2 Table 2 was entered into the mathematical optimization model as described in section 3.2 with the objective function using a standard deviation of all data roll decay, where the initial variables are $x_1 = 0.1$ m and $x_2 = B_{44} = 0.0001$ m-ton-sec. Result optimization can be found in the solid orange curve Fig. 3, and the fourth row Table 2. From the optimization calculation using all experimental data records obtained following the variables: $x_1 = 0.104727$ m; $x_2 = B_{44}$ =3.72067E-05 m-ton-sec; minimization of objective function σ =1.263851794; and constraint $1.2\Delta(0.078)^2 < 1.2\Delta(0.104726673)^2 < 1.2\Delta(0.156)^2$ fulfilled. The initial variables compare with the result variables; there are distinction

4.2 The objective function uses roll decay, a standard deviation of amplitude maximum-minimum

The second discussion is taken all 150 data records, the same as the first discussion, but the objective function calculation is different. However, the objective function employs a standard deviation of the maximum and minimum amplitudes with the time range 0-5.01 seconds obtained 25 data (13 maximum amplitude and 12 minimum amplitude). The comparison of the roll decay curves of experimental and optimization is shown in Fig. 4 as follows:

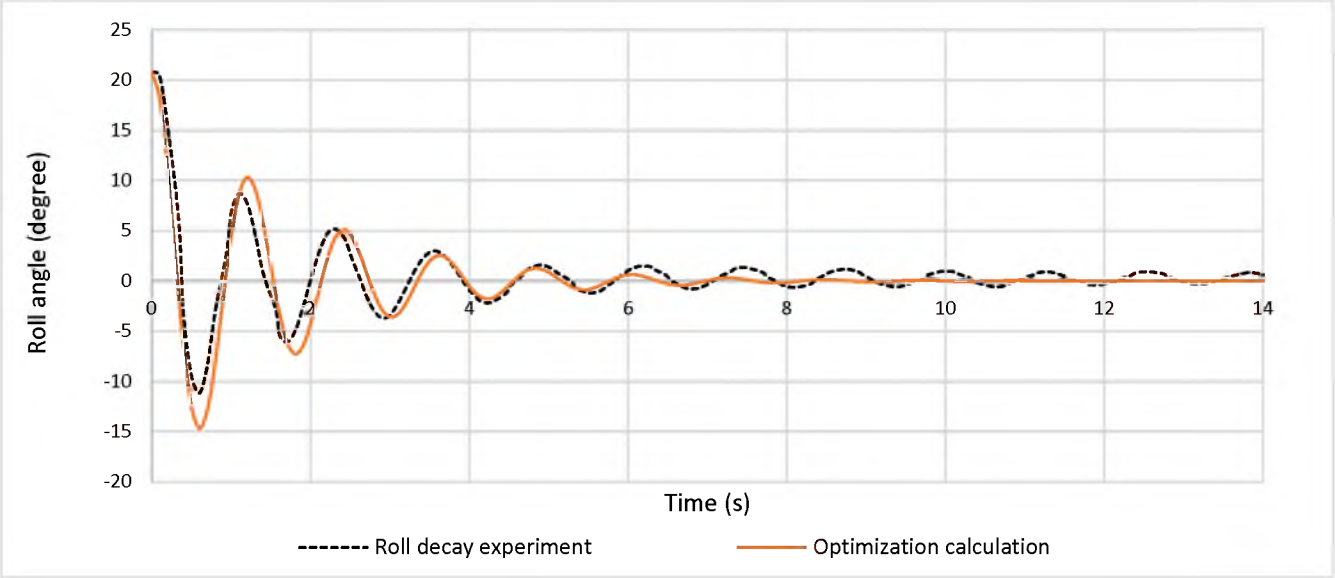

Fig. 4. Comparison of experiment with optimization using the objective function a standard deviation of amplitude maximum-minimum

From the graph in Fig. 4, curves are similar at the beginning to 0.503 seconds but are slightly different at 0.503-3.627 seconds. The curves return to experience the sameness at 3.627-6.044 seconds but are slightly different over time. Comparison curves of the experiment and optimization with the objective functions of the standard deviation of the maximum and minimum amplitude are also shown in Table 3. The first line shows the amount of data, the second line shows the data range of the gyrocompass recording time, and the third line shows the maximum and minimum amplitude data. The results of the roll decay optimization calculation are shown in Table 3, the solid orange curves and the third 3-row table as follows:

Table 3. Comparison of experiment with optimization using the objective function a standard deviation of amplitude maximum-minimum

Data (n)	1	2	3	4	5	6	7	.....	25
t (s)	0	0.604	1.108	1.712	2.317	2.921	3.526	.....	15.01
$\theta_{i.exp}$(deg)	20.830	-11.162	8.701	-6.075	5.153	-3.7244	2.9279	.....	0.6757
$\theta_{i.cal}$(deg)	20.830	-14.663	8.898	-6.193	4.317	-3.0571	2.1517	.....	-0.0026

Next is the determination of the initial variable value in the optimization calculation. The initial variable values are set up as the same in the discussion of section 4.1, but the objective function is the difference using amplitude maximum-minimum. Table 3, n is a set of data recorded, t is a set of time recorded from the gyroscope, $\theta_{i.exp}$ is a set of times recorded from the gyroscope, and $\theta_{i.cal}$ is a set of times recorded from the gyroscope. From the results of the optimization calculation, obtained the optimum variable: $x_1 = 0.1087688$ m; $x_2 = B_{44}$ = 3.00306E-05 m-ton-sec. Minimization of the objective function obtained $\sigma = 1.006776$ and constraint $1.2\Delta(0.078)^2 < 1.2\Delta(0.108768874)^2 <$

$1.2\Delta(0.156)^2$ fulfilled. When compared to the difference in the value of the variable in section 4.1, there is a difference Δx_1 =3,72% and Δx_2 =23.90%.

4.3 The objective function uses roll decay, a standard deviation of amplitude maximum

The third discussion is taken all 150 data records, the same as the first and the second discussion, but the objective function calculation is different. However, the objective function employs a standard deviation of the maximum and minimum amplitudes with a time range of 0-15.01 seconds, obtaining 13 maximum amplitudes. The comparison of the roll decay curves of experimental and optimization is shown in Fig. 5 as follows:

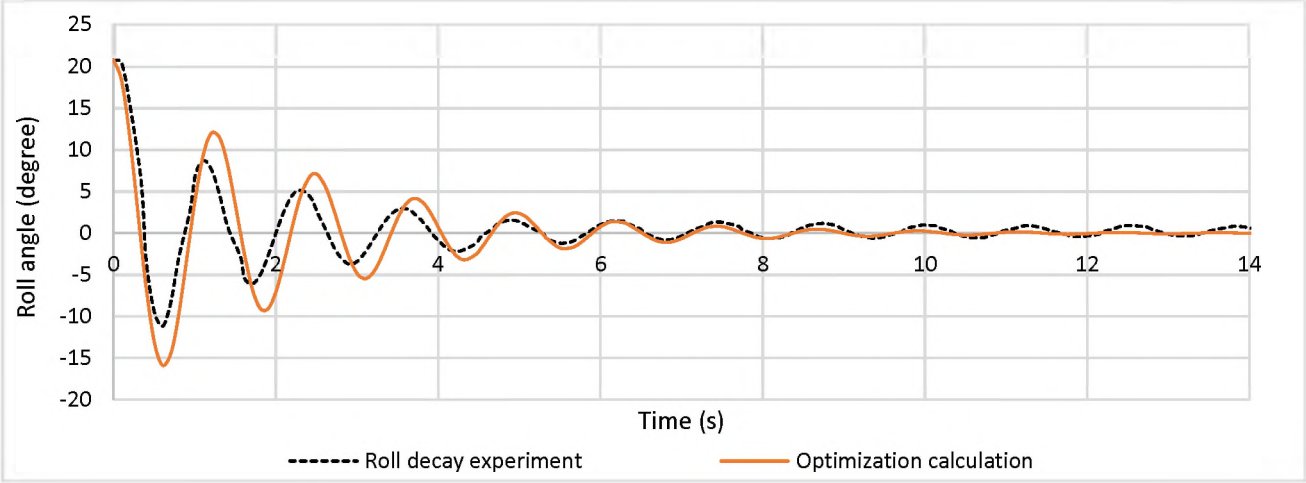

Fig. 5. Comparison of experiment with optimization using the objective function a standard deviation of amplitude maximum

The results of the optimization calculation compared to the experiment in Fig. 5 have the same initial roll setting value at the beginning to 0.503 seconds but are slightly different at 0.503-5.333 seconds. The curves return to experience the sameness at 5.333-9.167 seconds but are slightly different over time. In addition to comparing experimental and optimization results displayed in curves, it can also be displayed in the form of data, as shown in Table 4.

Table 4. Comparison of experiment with optimization using the objective function a standard deviation of amplitude maximum

Data (n)	1	2	3	4	5	6	7	.....	13
t (s)	0	1.108	2.317	3.526	4.937	6.145	7.464	.....	15.01
$\theta_{i.exp}$(deg)	20.830	8.7012	5.1526	2.9279	1.5491	1.4557	1.3458	.....	0.6757
$\theta_{i.cal}$(deg)	20.830	9.5125	4.8094	2.296	2.440	1.394	0.8263	.....	0.0245

Next is determining the initial variable value in the optimization calculation, where the initial variable value $x_2 = B_{44} = 0.0002$ m-ton-sec differs from sections 4.1, and 4.2, and we set the objective function at the amplitude maximum. From the results of the optimization calculation, we obtain the optimum variable: $x_1 = 0.108769$ m; $x_2 = B_{44}$ = 2.34841E-05 m-ton-sec. minimization of objective function $\sigma =$ 0.712748095 and constraint $1.2\Delta(0.078)^2 < 1.2\Delta(0.11129688)^2 < 1.2\Delta(0.156)^2$ fulfilled. When compared to the difference in the value of the variable in section 4.1, there is a $\Delta x_1 =$ 5.90% and $\Delta x_2 =$ 58.41%.

4.4 The objective function uses roll decay, a standard deviation of amplitude minimum

The third discussion is taken all 150 data records, the same as the first, second, and third discussions, but the objective function calculation is different. However, the objective function employs a standard deviation of the maximum and minimum amplitudes with a time range of 0-15.01 seconds, obtaining 12 minimum amplitudes. The comparison of the roll decay curves of experimental and optimization is shown in Fig. 6 as follows:

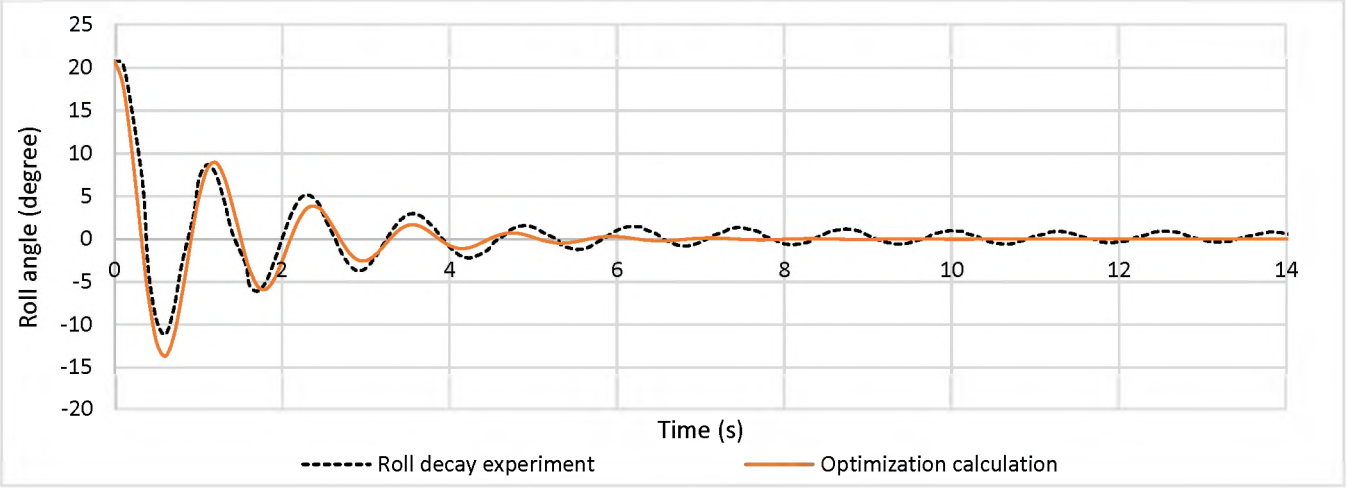

Fig. 6. Comparison of experiment with optimization using the objective function a standard deviation of amplitude minimum

From the graph in Fig. 6, peaks and valleys of amplitude are similar at the beginning to 0-2.015 seconds, different at 2.015-5.9144 seconds, but are slightly different at times above that range. The results of the data sorting of the minimum amplitude of objective functions are shown in Table 5: The first line shows the amount of data, the second line shows the data range of the gyrocompass recording time, and the third line shows the maximum and minimum amplitude data. The results of the roll decay optimization calculation are shown in Fig. 6 in the solid orange curves and the third 3-row table as follows:

Table 5. Comparison of experiment with optimization using the objective function a standard deviation of amplitude minimum

Data (n)	1	2	3	4	5	6	7	…..	12
t (s)	0.604	1.712	2.921	4.233	5.541	6.859	8.063	…..	14.507
$\theta_{i.exp}$(deg)	-11.162	-6.075	-3.724	-2.197	-1.209	-0.7745	-0.6317	…..	-0.2582
$\theta_{i.cal}$(deg)	-13.677	-5.531	-2.488	-1.010	-0.247	0.0114	0.0115	…..	0.0002

Next is the determination of the initial variable value in the optimization calculation. We equate the initial variable values with the value in the discussion of sections 4.1, 4.2, 4.3, and the objective function using amplitude maximum-minimum. From the results of the optimization calculation, we obtain the optimum variable: x_1 = 0.106631 m; x_2 = B_{44} = 3.50457E-05 m-ton-sec. Minimization of objective function σ = 1.068226721 and constraint $1.2\Delta(0.078)^2 < 1.2\Delta(0.106630962)^2 < 1.2\Delta(0.156)^2$ fulfilled. When compared to the difference in the value of the variable in section 4.1, there is a difference Δx_1=1.79% and Δx_2= 6.17%.

4.5 Optimization sensitivity analysis of hydrodynamic coefficients

Sensitivity is a critical analysis to determine the level of sensitivity of the initial variable input changes to the objective function entered into the calculation. This analysis determines that the stuck of the objective function at the optimum local peak can not occur. The aim is to cover the weaknesses of the GRG optimization method. This paper analyzes the sensitivity of the initial variables x_1 and x_2 to the optimal final variable. Where in the first part, the initial variable x_1 is made several variations and x_2 is made fixed, as shown in Table 6 below:

Table 6. Optimized sensitivities on k_{44} varied and B_{44} fixed

The objective function is a standard deviation of						
	k_{44}	0.1	0.2	0.3	0.4	0.5
	B_{44}	0.00001	0.00001	0.00001	0.00001	0.00001
All data roll decay	k_{44}	0.104727	0.104727	0.104727	0.104726	0.104726
	B_{44}	3.721E-05	3.721E-05	3.721E-05	3.721E-05	3.721E-05
Amplitude maximum-minimum	k_{44}	0.108769	0.108769	0.108769	0.108769	0.108769
	B_{44}	3.003E-05	3.003E-05	3.003E-05	3.003E-05	3.003E-05
Amplitude maximum	k_{44}	0.078000	0.111274	0.078000	0.000000	0.078000
	B_{44}	58.641463	819.20001	58.641463	0.00001	58.641463
Amplitude minimum	k_{44}	0.106631	0.106631	0.106631	0.106631	0.106631
	B_{44}	3.505E-05	3.505E-05	3.505E-05	3.505E-05	3.505E-05

Table 6 above the first row is the initial input variable from the optimization, which consists of variations k_{44}= (0.1; 0.2; 0.3; 0.4; 0.5) meters, while B_{44} = 0.0001 m-ton-sec is a fixed variable. The first column consists of four data variations used in the optimization as an objective function using a standard deviation: all data, maximum-minimum amplitude, maximum amplitude, and minimum amplitude. In the objective function with all data records, the optimal value obtained is k_{44} = 0.14727 m and B_{44} = 3.721E-05 m-ton-sec for the sensitivity of all initial variables is zero. As well as the objective function with maximum-minimum amplitude, the optimal value obtained is k_{44} = 0.108769 m dan B_{44} = 3.003E-05m-ton-sec for the sensitivity of all initial variables is zero too. While in optimization using maximum amplitude data, the optimal values of (k_{44} and B_{44}) are variable / very sensitive; on the other hand, the shape of roll decay is not the same pattern as the experiment. In the objective function with all data records, the optimal value obtained is k_{44} = 0.106631 m dan B_{44} = 3.505E-05 m-ton-sec for the sensitivity of all initial variables is zero. In the optimization of maximum amplitude, all optimization results are marked in red for all variations of the initial variable value k_{44}, because they produce a divergent curve where the shape of the optimization results curve differs from the roll decay of the experimental results.

Table 7. Optimized sensitivities on k_{44} fixed and B_{44} varied

The objective function is a standard deviation of						
	k_{44}	0.1	0.1	0.1	0.1	0.1
	B_{44}	0.00001	0.00002	0.00003	0.00004	0.00005
All data roll decay	k_{44}	0.104727	0.104727	0.104727	0.104727	0.104727
	B_{44}	3.721E-05	3.721E-05	3.721E-05	3.721E-05	3.721E-05
Amplitude maximum-minimum	k_{44}	0.108769	0.108769	0.108769	0.108769	0.104727
	B_{44}	3.003E-05	3.003E-05	3.003E-05	3.003E-05	3.721E-05
Amplitude maximum	k_{44}	0.078000	0.111294	0.111299	0.111302	0.111304
	B_{44}	58.64146	2.349E-05	2.348E-05	2.351E-05	2.348E-05
Amplitude minimum	k_{44}	0.106631	0.106631	0.106631	0.106631	0.106631
	B_{44}	3.505E-05	3.505E-05	3.505E-05	3.505E-05	3.505E-05

Table 7 above k_{44}= 0.1 m fixed and variable B_{44}= (0.00001; 0.00002; 0.00003; 0.00004; 0.00055) m-ton-sec. There is no sensitivity or zero in the objective function using all data and optimization using minimum amplitude data. In the objective function using the initial maximum-minimum amplitude of the variable B_{44} = (0.00001~0.0004) m-ton-sec, there is no sensitivity but B_{44}= 0.00005 m-ton-sec there is sensitivity. Meanwhile, in the objective function of the maximum amplitude, sensitivity occurs in all variations, especially at B_{44} = 0.00001 m-ton-sec or does not make a roll decay graph similar to an experiment after increasing the initial variable B_{44} sensitivity occurs with a small value. In maximum amplitude optimization, all optimization results are marked in red for the initial variable value variation B_{44}= 0.0001, because it produces a divergent curve where the shape of the optimization curve is different from the roll decay of the experimental results, while the other initial variable values have convergent values.

5 CONCLUSIONS

The hydrodynamic coefficient of roll motion is needed in predicting dynamic ship stability and capsize. The coefficients can be obtained from roll decay in calm water experimental. The GRG optimization method can find these coefficients accurately and quickly by determining the components of the optimization variable: k_{44} and B_{44}; the objective function of the minimum standard deviation; constrained the radius of gyration applied to the ship roll motion. From discusses above, optimization using several objective functions: a standard deviation of all data, maximum-minimum amplitude, maximum amplitude, and minimum amplitude has a similarity curve with the experiment of roll decay. The most different form of the curve with the experiment of roll decay is optimization using the objective function of a standard deviation of amplitude maximum with value σ = 0.712748095. The closest form of the curve with the experimentation of roll decay is optimization using the objective function of a standard deviation of amplitude maximum-minimum with value σ = 1.006776445. The optimum variables of hydrodynamic coefficients obtained are: x_1 = 0.108769 m; $x_2 = B_{44}$ = 3.00306E-05 m-ton-sec. In general, the GRG optimization method is usable in the search for the hydrodynamic coefficient of the roll decay, which has the advantage of having an accurate and fast value.

6 ACKNOWLEDGMENTS

We acknowledge the Directorate of Research and Community Service-ITS, which has provided financial support. Moreover, Alaik Nur Wahyudi-Indonesia's National Transportation Safety Committee (NTSC) helped provide data on the RoPax ship. Furthermore, the Flume Tank Laboratory of the Ocean Engineering Department-ITS conducted ship model experiments.

7 REFERENCES

[1] L. Sciberras and J. R. Silva, "The UN's 2030 Agenda for sustainable development and the maritime transport domain: the role and challenges of IMO and its stakeholders through a grounded theory perspective," *WMU J Marit Affairs*, vol. 17, no. 3, pp. 435–459, Sep. 2018, doi: 10.1007/s13437-018-0147-2.

[2] T. R. Walker *et al.*, "Chapter 27 - Environmental Effects of Marine Transportation," in *World Seas: an Environmental Evaluation (Second Edition)*, C. Sheppard, Ed. Academic Press, 2019, pp. 505–530. [Online]. Available: https://www.sciencedirect.com/science/article/pii/B9780128050521000309

[3] Z. Zhang and X.-M. Li, "Global ship accidents and ocean swell-related sea states.," *Natural Hazards & Earth System Sciences*, vol. 17, no. 11, 2017.

[4] H. Hasanudin, A. Zubaydi, and W. D. Aryawan, "Stability Assessments of RoPax Open Car Deck on Longitudinal Wave," *IOP Conf. Ser.: Earth Environ. Sci.*, vol. 1081, no. 1, p. 012031, Sep. 2022, doi: 10.1088/1755-1315/1081/1/012031.

[5] N. Baird, "Fatal ferry accidents, their causes, and how to prevent them," *(Doctor of Philosophy thesis, Australian National Centre for Ocean Resources and Security, University of Wollongong*, Jan. 2018, [Online]. Available: https://ro.uow.edu.au/theses1/498

[6] H. Kim, S. Haugen, and I. B. Utne, "Assessment of accident theories for major accidents focusing on the MV SEWOL disaster: Similarities, differences, and discussion for a combined approach," *Safety science*, vol. 82, pp. 410–420, 2016.

[7] A. Christodoulou, Z. Raza, and J. Woxenius, "The integration of RoRo shipping in sustainable intermodal transport chains: The case of a North European RoRo service," *Sustainability*, vol. 11, no. 8, p. 2422, 2019.

[8] K. Formela, T. Neumann, and A. Weintrit, "Overview of Definitions of Maritime Safety, Safety at Sea, Navigational Safety and Safety in General," *TransNav*, vol. 13, no. 2, pp. 285–290, 2019, doi: 10.12716/1001.13.02.03.

[9] P. R. Alman, "Thoughts on Integrating Stability into Risk Based Methods for Naval Ship Design," in *Contemporary Ideas on Ship Stability*, vol. 119, V. L. Belenky, K. J. Spyrou, F. van Walree, M. Almeida Santos Neves, and N. Umeda, Eds. Cham: Springer International Publishing, 2019, pp. 927–944. doi: 10.1007/978-3-030-00516-0_55.

[10] Y. Yang, B. Zhang, C. Zeng, X. Lu, and S. Chen, "Review of Research Status and Development of Paralysis Ship Stability Criteria," *International Journal of Science*, vol. 7 No.6, 2020.

[11] J. Rahola, *The Judging of the Stability of Ships and the Determination of the Minimum Amount of Stability–Especially Considering the Vessels Navigating Finnish Waters*. Aalto University, 1939.

[12] P. Ruponen, "Rahola criterion revisited: an overview of Jaakko Rahola's research and career," in *Proceedings of the 17th International Ship Stability Workshop ISSW2019, Helsinki, Finland*, 2019, pp. 15–20.

[13] D. Paroka and S. Asri, "Alternative Assessment of Weather Criterion For Ships With Large Breadth And Draught Ratios By A Model Experiment: A Case Study On An Indonesian RO-RO Ferry," *International Journal of Maritime Engineering*, vol. 162, no. A1, Art. no. A1, 2020.

[14] A. Ariffin, S. Mansor, and J.-M. Laurens, "A Numerical Study for Level 1 Second Generation Intact Stability Criteria," 2015, pp. 183–193.

[15] A. Francescutto, "Intact stability criteria of ships – Past, present and future," *Ocean Engineering*, vol. 120, pp. 312–317, Jul. 2016, doi: 10.1016/j.oceaneng.2016.02.030.

[16] W. Peters and V. Belenky, "Regulatory Aspects of Implementation of IMO second generation intact stability criteria," 2016, pp. 13–15.

[17] N. Petacco and P. Gualeni, "IMO Second Generation Intact Stability Criteria: General Overview and Focus on Operational Measures," *JMSE*, vol. 8, no. 7, p. 494, Jul. 2020, doi: 10.3390/jmse8070494.

[18] J. Lister, "Green Shipping: Governing Sustainable Maritime Transport," *Global Policy*, vol. 6, no. 2, pp. 118–129, May 2015, doi: 10.1111/1758-5899.12180.

[19] P. IMO, "Background of criteria regarding righting lever curve properties (part A of the 2008 IS Code)," 2008. https://www.imorules.com/GUID-E8AD1425-5B54-4291-AF02-184A91FE1C2B.html (accessed Jul. 19, 2022).

[20] T. Kubo, N. Umeda, S. Izawa, and A. Matsuda, "Total Stability Failure Probability of a Ship in Beam Wind and Waves: Model Experiment and Numerical Simulation," in *Contemporary Ideas on Ship Stability*, vol. 119, V. L. Belenky, K. J. Spyrou, F. van Walree, M. Almeida Santos Neves, and N. Umeda, Eds. Cham: Springer International Publishing, 2019, pp. 591–603. doi: 10.1007/978-3-030-00516-0_35.

[21] C. A. Rodríguez, I. S. Ramos, P. T. Esperança, and M. C. Oliveira, "Realistic estimation of roll damping coefficients in waves based on model tests and numerical simulations," *Ocean Engineering*, vol. 213, p. 107664, 2020.

[22] C.-J. Söder, A. Rosén, S. Werner, M. Huss, and J. Kuttenkeuler, "Assessment of Ship Roll Damping Through Full Scale and Model Scale Experiments and Semi-empirical Methods," in *Contemporary Ideas on Ship*

Stability, vol. 119, V. L. Belenky, K. J. Spyrou, F. van Walree, M. Almeida Santos Neves, and N. Umeda, Eds. Cham: Springer International Publishing, 2019, pp. 177–190. doi: 10.1007/978-3-030-00516-0_10.

[23] ITTC, "ITTC Quality System Manual Recommended Procedures and Guidelines Procedure Model Tests on Intact Stability." International Towing Tank Conference, 2008.

[24] M. Gu, J. Lu, S. Bu, C. Wu, and G. Qiu, "Numerical simulation of the ship roll damping," *Proceedings of STAB*, pp. 341–348, 2015.

[25] A. Oliva-Remola and L. Pérez-Rojas, "A step forward towards developing an uncertainty analysis procedure for roll decay tests," in *Proceedings of the 17th International Ship Stability Workshop, Helsinki*, 2019.

[26] S. Dissanayake and T. Rupasinghe, "Warehouse Optimization using Generalized Reduced Gradient (GRC) Method," in *11th Annual International Conference on Industrial Engineering and Operations Management (Singapore)*, 2021, pp. 1–12.

[27] R. Subramanian and P. V. Jyothish, "Genetic algorithm based design optimization of a passive anti-roll tank in a sea going vessel," *Ocean Engineering*, vol. 203, p. 107216, 2020.

[28] A. Msabawy and F. Mohammad, "Continuous sizing optimization of cold-formed steel portal frames with semi-rigid joints using generalized reduced gradient algorithm," *Materials Today: Proceedings*, vol. 42, pp. 2290–2300, 2021, doi: 10.1016/j.matpr.2020.12.318.

[29] M. N. Nawaz *et al.*, "Cost-Based Optimization of Isolated Footing in Cohesive Soils Using Generalized Reduced Gradient Method," *Buildings*, vol. 12, no. 10, p. 1646, Oct. 2022, doi: 10.3390/buildings12101646.

[30] M. Jalal and M. Goharzay, "Cuckoo search algorithm for applied structural and design optimization: Float system for experimental setups," *Journal of Computational Design and Engineering*, vol. 6, no. 2, pp. 159–172, Apr. 2019, doi: 10.1016/j.jcde.2018.07.001.

[31] J. Lu, M. Gu, and E. Boulougouris, "Model experiments and direct stability assessments on pure loss of stability in stern quartering waves," *Ocean Engineering*, vol. 216, p. 108035, Nov. 2020, doi: 10.1016/j.oceaneng.2020.108035.

[32] C. A. Rodríguez and M. A. S. Neves, "Investigation on Parametrically Excited Motions of Spar Platforms in Waves," in *Contemporary Ideas on Ship Stability*, vol. 119, V. L. Belenky, K. J. Spyrou, F. van Walree, M. Almeida Santos Neves, and N. Umeda, Eds. Cham: Springer International Publishing, 2019, pp. 291–305. doi: 10.1007/978-3-030-00516-0_17.

E. Uzunoglu and C. Guedes Soares, "Automated processing of free roll decay experimental data," *Ocean Engineering*, vol. 102, pp. 17–26, Jul. 2015, doi: 10.1016/j.oceaneng.2015.04.016.

[33] V. Belenky and N. B. Sevastianov, *Stability And Safety of Ships Risk of Capsizing*, The Society of Naval Architects and Marine Engineers (SNAME)., vol. Second Edition. 2007.

[34] R. Bhattacharyya, *Dynamics of marine vehicles*. Wiley Series in Computing, 1978.

[35] C. Walha and A. M. Alimi, "Human-like modeling and generation of grasping motion using multi-objective particle swarm optimization approach," *International Journal of Computer Science and Information Security*, vol. 14, no. 8, p. 694, 2016.

[36] R. Y. M. Li and A. Chan, "Reits Portfolio Optimization: A Nonlinear Generalized Reduced Gradient Approach," in *International Conference on Modeling, Simulation and Optimization*, 2018, pp. 216–223.

[37] R. S. Correia, G. F. F. Bono, and G. Bono, "Optimization of reinforced concrete beams using Solver tool," *Rev. IBRACON Estrut. Mater.*, vol. 12, no. 4, pp. 910–931, Aug. 2019, doi: 10.1590/s1983-41952019000400011.

Paper submitted: 29.09.2022.

Paper accepted: 23.12.2022.